J Solid State Electrochem (2012) 16:1925–1931
DOI 10.1007/s10008-011-1585-3

ORIGINAL PAPER

Oxalic acid-assisted preparation of $LiFePO_4$/C cathode material for lithium-ion batteries

Junqing Dou · Xueya Kang · Tuerdi Wumaier · Ning Hua · Ying Han · Guoqing Xu

Received: 31 August 2011 / Revised: 16 October 2011 / Accepted: 30 October 2011 / Published online: 26 November 2011

Abstract $LiFePO_4$/C composite is synthesized by oxalic acid-assisted rheological phase method. Fe_2O_3 and LiH_2PO_4 are chosen as the starting materials, sucrose as carbon sources, and oxalic acid as the additive. The crystalline structure and morphology of the products are characterized by X-ray diffraction and field emission scanning electron microscopy. The charge–discharge kinetics of $LiFePO_4$ electrode is investigated using cyclic voltammetry and electrochemical impedance spectroscopy. It is found that the introduction of appropriate amount of oxalic acid leads to smaller particle sizes, more homogeneous size distribution, and some Fe_2P produced in the final products, resulting in reduced polarization, impedance, and improved Li^+ ion diffusion coefficient. The best cell performance is delivered by the sample with R=1.5 (R of the molar ratio of oxalic acid to LiH_2PO_4). Its discharge capacity is 154 mAh g^{-1} at 0.2 C rate and 120 mAh g^{-1} at 5.0 C rate. At the same time, it exhibits an excellent cycling stability; no obvious decrease even after 1,000 cycles at 1.0 C rate.

Keywords Oxalic acid · Cathode · Lithium iron phosphate · Li-ion batteries

J. Dou · X. Kang · T. Wumaier · N. Hua · Y. Han · G. Xu
Xinjiang Technical Institute of Physics and Chemistry,
Chinese Academy of Sciences,
Urumqi, Xinjiang 830011, China

J. Dou
Graduate University of Chinese Academy of Sciences,
Beijing 100049, China

J. Dou · X. Kang (✉) · T. Wumaier · N. Hua · Y. Han · G. Xu
Xinjiang Key Laboratories of Electronic
Information Materials and Devices,
Urumqi, Xinjiang 830011, China
e-mail: xueyakang@yahoo.cn

Introduction

Since the pioneering work of Padhi and co-workers in 1997 [1], olivine-structured lithium iron phosphate—$LiFePO_4$—has been recognized as a promising cathode material for lithium-ion batteries. Compared with other cathode materials, $LiFePO_4$ exhibits the advantages of high theory capacity (~170 mAh g^{-1}), excellent thermal stability, no toxicity and low cost, high reversibility, etc. However, its intrinsic low electronic conductivity (~10^{-9} S cm^{-1}) and low Li^+ ion conductivity (~2×10^{-14} cm^2 S^{-1}) limit the rate capability and then its application. Many efforts have been tried to solve these problems, such as coating some conductive materials on the surface of the particles, doping some cations or anions into the structure and minimizing the particle size, etc. [2–4].

$LiFePO_4$ is usually prepared by solid-state carbon thermal reduction, sol–gel method, hydrothermal method, co-precipitation, and rheological phase method [5–9]. Rheological phase method is favorable to synthesize small pure products and well-distributed particles. Firstly, the solid reactants are fully mixed in a proper molar ratio. Then, add a proper amount of water or other solvents in it and continue stirring or grinding until a uniform mixture (rheological phase mixture) was obtained. The solid powders and liquid substances are uniformly distributed in the mixture, so the surface area of the solid particles can be utilized more efficiently than that in the solid-state phase. And then the mixture reacted in an appropriate condition to get the precursor. Finally, the target product can be obtained after appropriate sintering treatment process. The process is simple and cheap due to no need of ball milling. Many other materials have been prepared via rheological method. Ren et al. [10] has reported that the $LiNi_{1/3}Co_{1/3}Mn_{1/3}O_2$ cathode material prepared by

rheological phase method exhibits better electrochemical performance than via conventional solid-state method owing to higher specific surface area, lower cation mixing, higher reversible discharge capacity, and better cycling stability. Cheng et al. [11] also prepared $LiNi_{0.65}Co_{0.25}Mn_{0.1}O_2$ cathode material via rheological phase method. The results showed that the prepared powders have a higher ordered layer $NaFeO_2$ structure, smaller particle size, and lager surface area, which are all favorable for electrochemical performances. Therefore, the prepared material exhibited better electrochemical performances, such as lower cell polarization, lower surface layer resistance, higher reversible capacity, and better cycling stability. He et al. [12] obtained the tin oxide-based composite by rheological phase method. And the performance testing results showed that the prepared material has an average size of about 150 nm and well crystalline. At the same time, the sample delivers a high-charge capacity of more than 570 mAh g^{-1} and the capacity loss per cycle is only about 0.15% after being cycled 30 times.

In addition, if some appropriate chelating agents or some agents that can react with the solid particles even in a small extent only were introduced, these would significantly improved the degree of mixing, even to the molecular level. Take oxalic acid for example, owing to contain hydroxyl (–OH), it could be as a chelating agent to synthesize some materials, as it has been reported [13]. Moreover, as an acid, oxalic acid can react with metal oxides such as Fe_2O_3 to produce some soluble salt. Therefore, by adding oxalic acid in rheological phase method (some experiments choose metal oxide as raw material), it effectively improves the uniformity of the mixture of raw materials and then better performance is obtained.

In this work, oxalic acid-assisted rheological phase method is introduced to synthesize $LiFePO_4$/C composite material. The effect of oxalic acid on the electrochemical properties of the $LiFePO_4$/C composite was investigated by X-ray diffractions (XRD), field emission scanning electron microscopy (FESEM), charge–discharge test, cyclic voltammetry (CV), and electrochemical impedance spectroscopy (EIS) in detail.

Experiments

Preparation of $LiFePO_4$/C composite

$LiFePO_4$/C composite was synthesized via oxalic acid-assisted rheological phase method. All the reagents used in the experiment were of analytical purity and used without further purification. The Fe_2O_3 and LiH_2PO_4 were chosen as the starting materials, sucrose as carbon sources, and oxalic acid as the additive. Firstly, stoichiometric Fe_2O_3, LiH_2PO_4, sucrose, and appropriate amount of oxalic acid were fully mixed in an agate mortar by grinding. Then, proper quantity of liquid (ethanol to deionized water = 1:1 in volume) was added to form a rheological phase mixture. And then the mixture reacted in an oven at 80 °C for about 6 h to obtain the final precursor. The precursor was sintered at 350 °C for 5 h and 700 °C for 10 h respectively, under N_2 gas flow. After cooling to room temperature, the $LiFePO_4$/C composite was obtained. The samples were named as S1, S2, S3, and S4 according to the different amount of oxalic acid (R of the molar ratio of oxalic acid to LiH_2PO_4 and R=0.0, 0.5, 1.5, and 2.5).

Characterization of $LiFePO_4$/C composite

The crystalline phase was analyzed using XRD (RINT-2500V, Rigaku Co.) with CuKα radiation (λ=1.5418 Å) in the range of $15^\circ \leq 2\theta \leq 75^\circ$ with a scanning rate of 2°/min. The particle morphologies of the prepared powders were determined by FESEM (SUPRA-55VP).

Cell assembly and electrochemical tests

Electrochemical performances of the prepared $LiFePO_4$/C composite were investigated by using CR2025 coin cell. The cathode was fabricated from a mixture of the as-synthesized powders, acetylene black, and polyvinylidene fluoride with a weight ratio 80:15:5 and the electrolyte was 1 M $LiPF_6$ in a mixture of ethyl carbonate, diethyl carbonate, and dimethyl carbonate (volume ratio 1:1:1). The slurry was then cast on an aluminum foil and dried at 120 °C overnight under vacuum. The cells (CR2025) were assembled in an argon-filled glove box using lithium metal foil as the counter electrode and microporous polypropylene sheet (Celgard 2400, Celgard Inc., USA) as the separator. The cells were charged and discharged between 2.3 and 4.3 V on a charge/discharge apparatus (BTS-51, Neware, China). CV and EIS were tested using a CHI650 electrochemical working station.

Results and discussion

Material characterizations

Figure 1 showed the XRD patterns of the as-prepared $LiFePO_4$/C via oxalic acid-assisted rheological phase method with different oxalic acid content. The diffraction peaks of the sample S1 can be indexed on the basis of the orthorhombic olivine-type structure (with the P*nma* space group) without second phase, whereas the patterns of the samples S2, S3, and S4 showed the second phase of Fe_2P (marked with stars) and Li_3PO_4 (marked with arrow) exists except for the main diffraction peaks of the

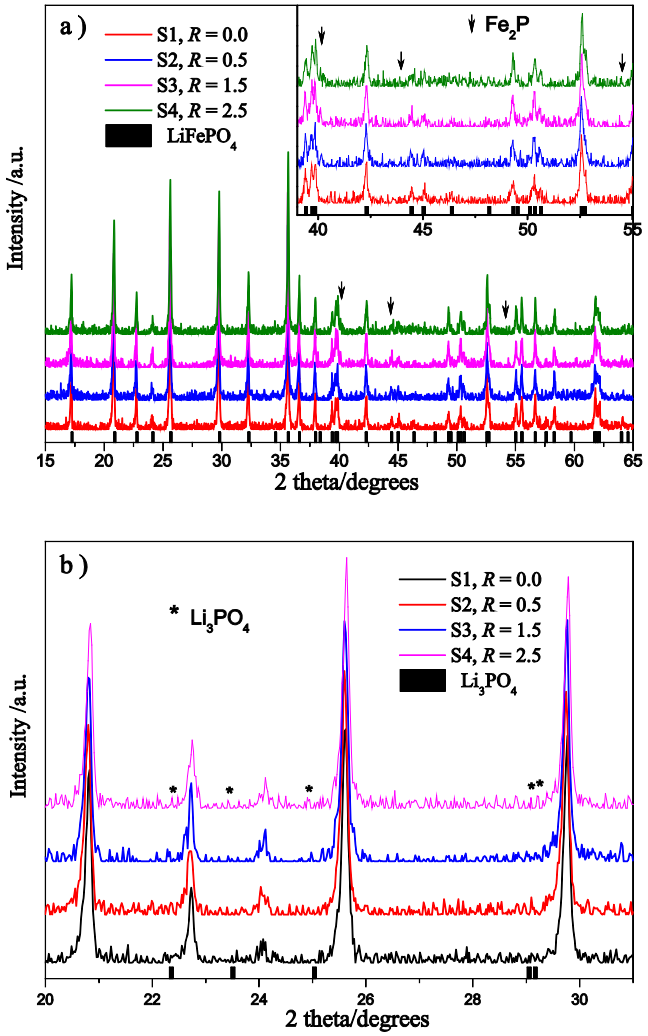

Fig. 1 XRD patterns of the samples S1, S2, S3, and S4

orthorhombic olivine structure $LiFePO_4$ (JCPDS 83-2092). The phenomenon of the Fe_2P and Li_3PO_4 diffraction peaks is not found in the XRD patterns of the sample S1 only, that means Fe_2P and Li_3PO_4 are generated mainly due to the added oxalic acid. In addition, there is no carbon diffraction peak found, indicating that the formed carbon may exist in amorphous state.

In fact, at high temperature, oxalic acid will be decomposed to a carbon monoxide and a water molecule, and then the H_2 will be generated as shown in reaction 1 [14]. Meantime, due to the presented H_2, a strong reducibility atmosphere will be introduced, and it can even reduce the $LiFePO_4$ to Fe_2P and Li_3PO_4 at high temperature. Therefore, some Fe_2P and Li_3PO_4 will be generated as shown in reaction 2 [15].

$$C_2H_2O_4 \xrightarrow[\text{High temp}]{} CO_2+CO+H_2O \xrightarrow[\text{High temp}]{} 2CO_2+H_2 \quad (1)$$

$$6LiFePO_4+16H_2 \xrightarrow[\text{High temp.}]{} 2Fe_2P+2Li_3PO_4 +2FeP+16H_2O \xrightarrow[\text{High temp}]{} 3Fe_2P+2Li_3PO_4+P \quad (2)$$

In addition, Nazar et al. [16] argued that a continuous "nanonetwork" of metal-rich phosphides on the surface of the $LiFePO_4$ particles can enhance electronic conductivity of the $LiFePO_4$ composite effectively because those metal phosphides usually exhibit high-electron conductivity. Therefore, the $LiFePO_4$/C composite prepared in the experiment with small amount of metal-rich phosphides—Fe_2P (the electron conductivity about 0.1–1.5 Scm^{-1} at room temperature [16–18]) may give a better electrochemical performance.

Since the morphology and particle sizes of $LiFePO_4$ have great influence on their electrochemical performance, FESEM analyses of these prepared samples were carried out. The FESEM images are shown in Fig. 2 with the same magnification. The sample S1 shows a wide size distribution from 200 nm to 1 μm. Samples S2 and S3 show smaller particles than S1 but also exhibit a wide size distribution and the sample S4 shows a relatively serious agglomeration. While the sample S3 exhibits the smallest particles (around 100 to 150 nm) and uniform distribution with the ellipsoid morphology, it is obvious that the introduced oxalic acid plays an important role in the morphology and distribution of the products. Generally, a smaller and uniformed distribution particle sizes allow easier penetration of the electrolyte and provide a shorter pathway for Li^+ ion diffusion in the active material that is favorable for Li^+ ion diffusion. It indicated that the sample S3 should have the better electrochemical performance than others.

Electrochemical properties

The charge–discharge curves of these samples (S1, S2, S3, and S4) between 2.3 and 4.3 V at 0.2 C rate are shown in Fig. 3. All samples show a flat and long voltage plateaus at about 3.45 V, which are the main characteristic of the two-phase reaction of $LiFePO_4$. The discharge capacities of samples S1, S2, S3, and S4 are 124, 139, 154, and 137 mAh g^{-1}, respectively. The sample S3 shows the lowest electrode polarization and longest flat voltage plateaus. The polarization potential of the as-synthesized samples S1, S2, S3, and S4 are 64, 59, 55, and 77 mV (inset of Fig. 3), respectively, indicating that the higher reaction kinetics of the sample S3. The results accord well with the previous reports [19, 20].

The results of the rate performance study for the cells comprised the prepared samples cycled with various C rates

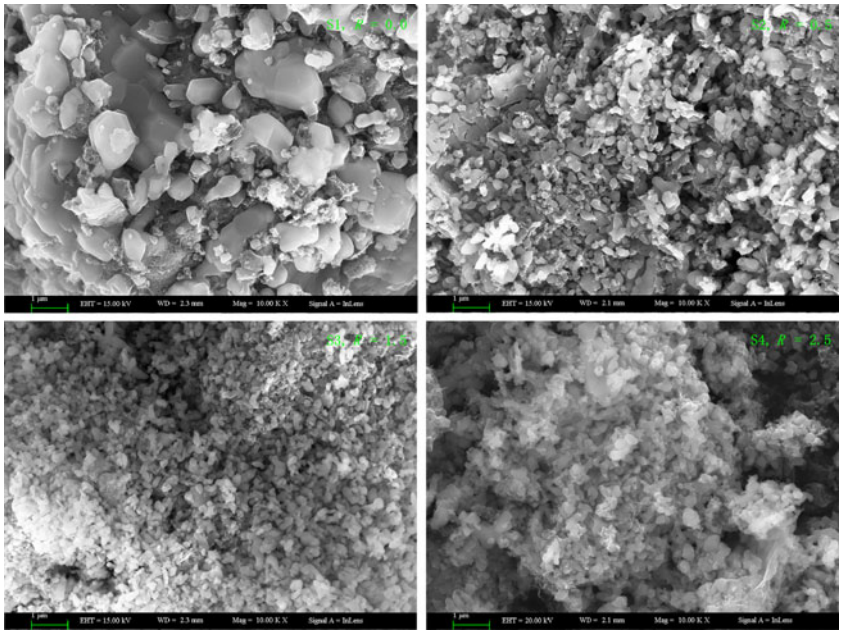

Fig. 2 FESEM images of the samples S1, S2, S3, and S4 with the same magnification

at room temperate are shown in Fig. 4. It clearly demonstrated that the sample S3 exhibits a better rate performance than others. It delivers a discharge capacity of 120 mAh g^{-1} even at 5.0 C rate, compared with 95, 103, and 101 mAh g^{-1} for the samples S1, S2, and S4 at the same rate, respectively. At the same time, when recovering the former testing current densities (1.0 C rate in the experiment), the discharge capacity of the sample S3 almost has no decrease, which indicates the stabled structure and good cyclic reversibility of the electrodes. In addition, the discharge capacity of the sample S3 has no obvious decrease even after 1,000 cycles at 1.0 C rate (inset of Fig. 4), which shows good cycling stability and capacity reversibility. The enhanced rate and cycling performances of the sample S3 are mainly attributed to the small and uniformed particles which results higher Li^+ ion diffusion coefficient as discussed above.

On the other hand, oxalic acid can react with Fe_2O_3 to produce same soluble salt ($H_3Fe(C_2O_4)_3$) as shown in the reaction 3. Therefore, the uniformity of the mixture of raw materials could be effectively improved. That also favors for improving the performances including higher discharge capacity, better rate performance, and better cycling stability.

$$Fe_2O_3 + 6H_2C_2O_4 \longrightarrow 2H_3Fe(C_2O_4)_3(\text{soluble, aquamarine}) + 3H_2O \quad (3)$$

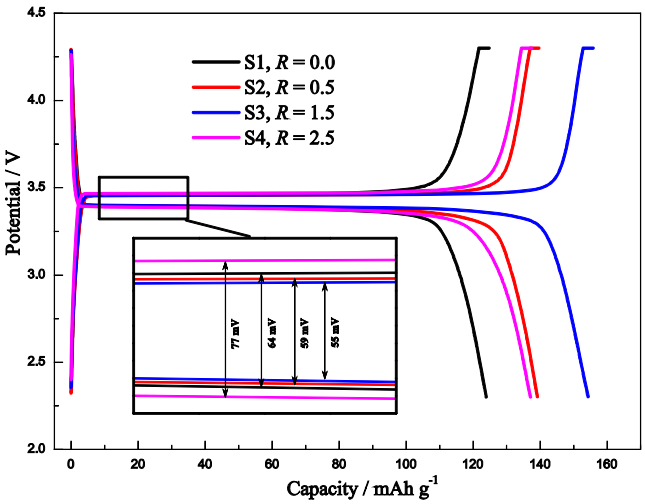

Fig. 3 The charge/discharge curves of the samples S1, S2, S3, and S4 at 0.2 C rate

Cyclic voltammetry tests

CV is a well-suited technique to evaluate the cathode performance and electrode kinetics of the oxide materials. The prepared $LiFePO_4$/C composite materials were tested at room temperature in the range of 2.3–4.3 V and the scan rate was 0.1 mV s^{-1}. As shown in Fig. 5, every sample exhibits a pair of redox peaks during testing, corresponding to the phase-transition process between $LiFePO_4$ and $FePO_4$. From the CV curves, the sample S3 exhibits the highest peak current and the smallest potential difference (ΔE) of the redox peaks, indicating that the fastest electrode reaction kinetics and the lowest electrode polarization consequently are the best electrochemical performance. The faster electrode reaction kinetics and the lower electrode polarization may be related to the small particle size and the presented small amount of Fe_2P in the sample S3.

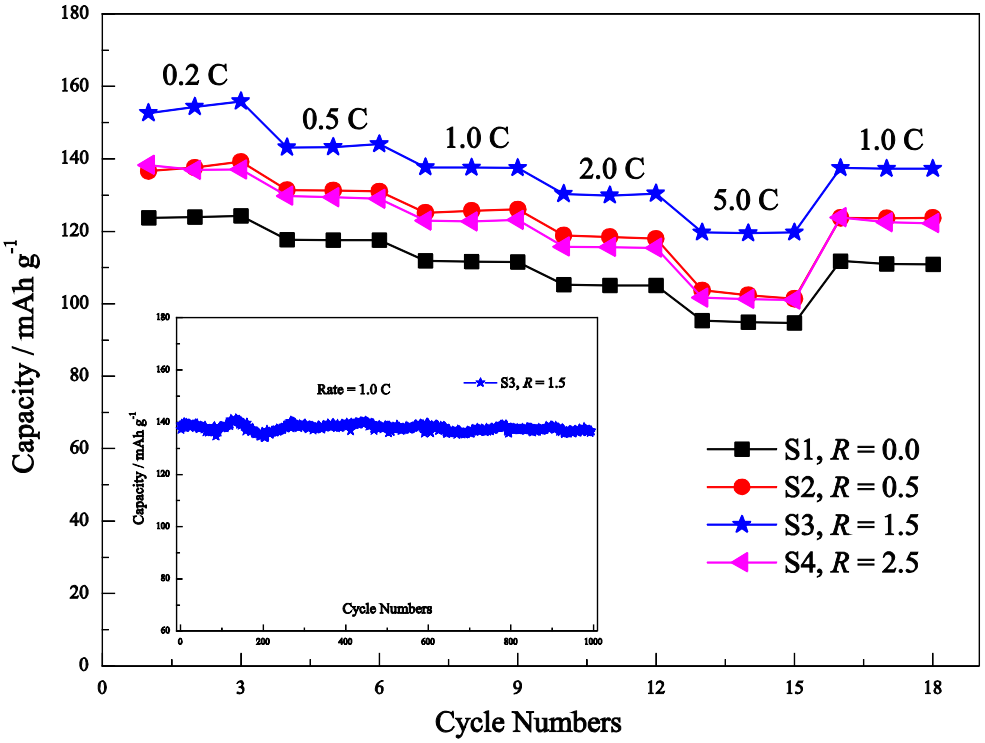

Fig. 4 The rate performance of the samples S1, S2, S3, and S4 with various C rates at room temperate and the cyclic curves of the sample S3 at 1.0 C rate

EIS measurements

To further understand oxalic acid effect on the kinetics process of the electrode materials, EIS measurements were carried out in a fully discharged coin cell (CR2025, 2.3 V). Figure 6 showed the EIS data of all the samples which synthesized with different content of oxalic acid. The Nyquist plots of these samples are all combined in one semicircle in high-to-medium frequency and in an inclined line in low frequency. Generally, the semicircle in high-to-medium frequency semicircle is attributed to the charge transfer resistance (R_{ct}), and the inclined line at low frequencies is attributed to Warburg impedance that is associated with Li^+ ion diffusion in electrodes. In the high-to-medium frequency region, the sample S3 exhibits the smallest R_{ct} (~23 Ω) than that of the sample S1 (~48 Ω), S2

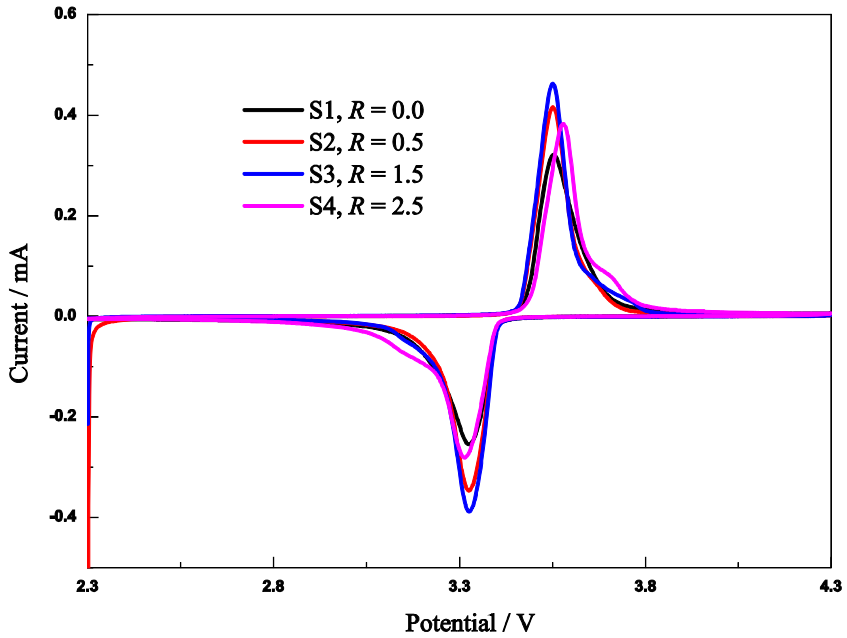

Fig. 5 The CVs plots of the four $LiFePO_4$/C composite materials at a scan rate of 0.1 mV s^{-1}

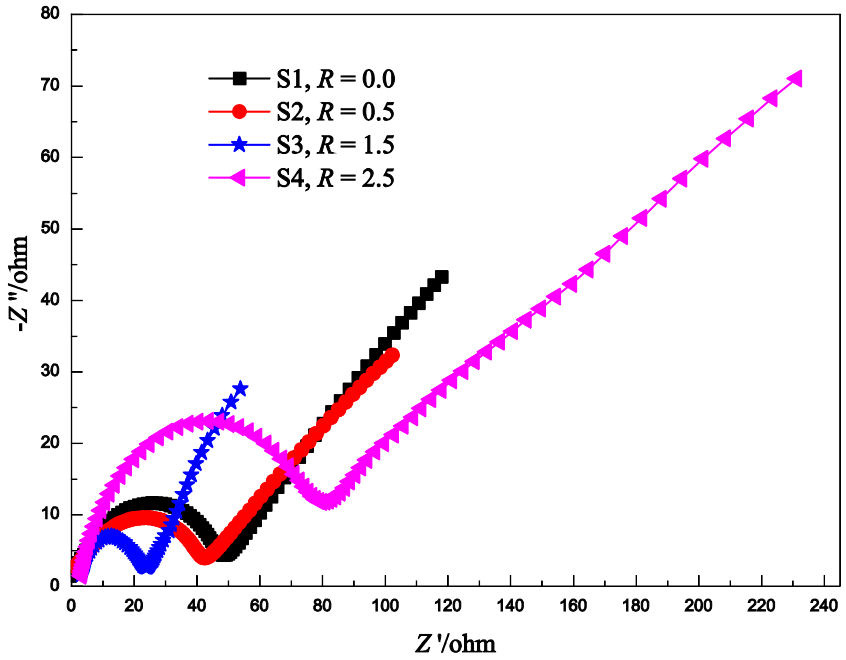

Fig. 6 The Nyquist plots of the fully discharged coin cell assembled with the samples S1, S2, S3, and S4 as cathode

(~43 Ω), and S4 (~80 Ω). The smallest R_{ct} value of the sample S3 indicates a lower electrochemical polarization, faster electrode/electrolyte interface reaction, and lithium diffusion processes. The lowest R_{ct} of the sample S3 may be due to the small particle size, uniform distribution particles, and the presence of Fe_2P which results in higher electron conductivity [18, 21].

In addition, according to the literatures [22, 23], the lithium diffusion coefficient can be calculated by the following two equations:

$$D_{Li} = \frac{R^2T^2}{2n^4F^4C^2\sigma^2} \tag{4}$$

$$Z' = \sigma\omega^{-\frac{1}{2}} \tag{5}$$

where D_{Li} is the Li^+ ion diffusion coefficient, R is the gas constant, T is the absolute temperature, n is the number of electrons per species reaction, F is the Faraday constant, C is the concentration of lithium ions, and σ is the Warburg

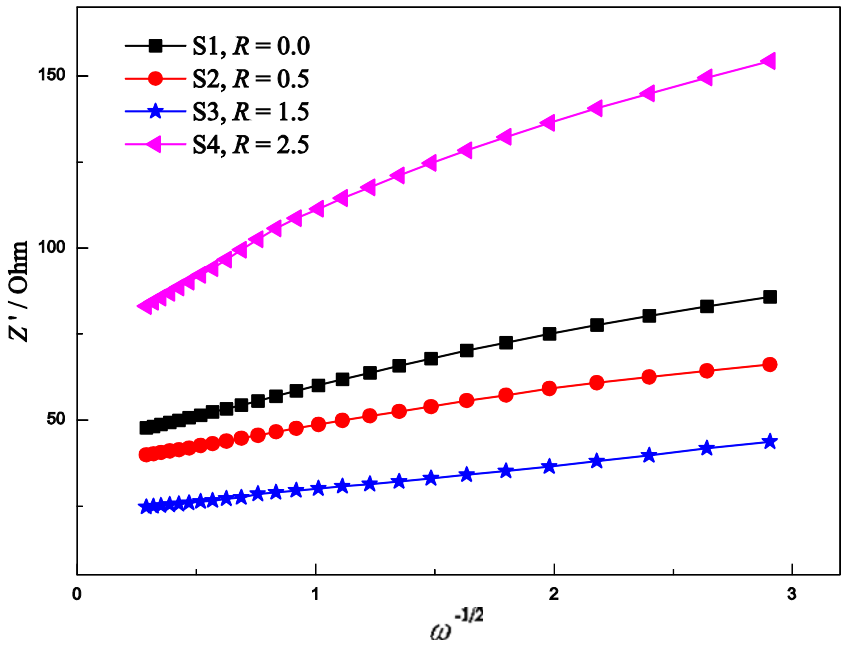

Fig. 7 The relationships between Z' and $\omega^{-1/2}$ for the samples S1, S2, S3, and S4

factor which could be obtained by Eq. 5. Thus, the Li^+ ion diffusion coefficient is inversely proportional to σ^2. Figure 7 shows the relationship between Z' and square root of frequency $\omega^{-1/2}$ in low-frequency region; the value of σ could be obtained from the slope. The calculated Li^+ ion diffusion coefficient of these samples are $D_{Li,\ S1}=3.20\times10^{-13}$ $cm^2\ S^{-1}$, $D_{Li,\ S2}=6.76\times10^{-13}$ $cm^2\ S^{-1}$, $D_{Li,\ S3}=1.29\times10^{-12}$ $cm^2\ S^{-1}$, and $D_{Li,\ S4}=9.15\times10^{-14}$ $cm^2\ S^{-1}$ based on Eqs. 4 and 5. Obviously, the sample S3 exhibits the maximum D_{Li}, which is two orders of magnitude larger than the pure $LiFePO_4$ ($\sim2\times10^{-14}$ $cm^2\ S^{-1}$) and is consistent well with the previous report by Fey et al. [24], who obtained the lithium-ion diffusion coefficient of 2.4×10^{-12} $cm^2\ S^{-1}$ for $LiFePO_4$ electrodes. The high D_{Li} of sample S3 is attributing to the small and uniform distribution particles which results in short lithium-ion diffusion distance.

In summary, the lowest polarization potential, impedance, and highest Li^+ ion diffusion coefficient of sample S3 are due to the small, uniform distribution, the improved degree of mixing between raw materials, and the presence of Fe_2P. These are all in favor for improving the electrochemical performances of $LiFePO_4$. Therefore, the high capacity, good rate performance, and cycling stability are obtained.

Conclusion

$LiFePO_4$/C composite is synthesized by oxalic acid-assisted rheological phase method. XRD and FESEM analysis indicate that the orthorhombic olivine structure $LiFePO_4$ (with ellipsoid morphology) is successfully prepared and some Fe_2P are introduced due to the added oxalic acid. The electrochemical performance testing results showed that the sample S3 with $R=1.5$ exhibits the best electrochemical performances due to the small particle sizes, uniform distribution particles, the improved degree of mixing between raw materials, and the presence of Fe_2P. Its discharge capacity is 154 mAh g^{-1} at 0.2 C rate and 120 mAh g^{-1} even at 5.0 C rate. At the same time, it exhibits an excellent cycling stability and no obvious decrease even after 1,000 cycles at 1.0 C rate. The obtained excellent electrochemical performance of the $LiFePO_4$/C composite should enable the wide acceptance and application in long-life lithium-ion batteries with high-power and high-energy density.

Acknowledgments This work was support by the West Light Foundation of the Chinese Academy of Sciences (no. XB200919), the Knowledge Innovation Program of the Chinese Academy of Sciences (no. 20092A401), and the science and technology projects of Urumqi (no. K111410005).

References

1. Padhi AK, Nanjundaswamy KS, Goodenough JB (1997) J Electrochem Soc 144:1188–1194
2. Shin HC, Nam KW, Chang WY (2011) Electrochim Acta 56:1182–1189
3. Liu H, Feng Y, Wang Z, Wang K, Xie JG (2008) Powder Technol 184:313–317
4. Zhang W, Hu Y, Tao X, Huang H, Gan YP, Wang CT (2010) J Phys Chem Solids 71:1196–1200
5. Liu YY, Cao CB, Li J (2010) Electrochim Acta 55:3921–3926
6. Liang GC, Wang L, Ou XQ, Zhao X, Xu SZ (2008) J Power Sources 184:538–542
7. Liu YY, Cao CB (2010) Electrochim Acta 55:4694–4699
8. Wang LN, Zhang ZG, Zhang KL (2007) J Power Sources 167:200–205
9. Kim JK, Cheruvally GR, Ahn JH (2008) J Solid State Electrochem 12:799–805
10. Ren HB, Wang YR, Li DC, Ren LH, Peng ZH, Zhou YH (2008) J Power Sources 178:439–444
11. Cheng CX, Tan L, Hu AZ, Liu HW, Huang XT (2010) J Alloys Compd 506:888–891
12. He ZQ, Li XH, Xiong LZ, Wu XM, Xiao ZB, Ma MY (2005) Mater. Chem Phys 93:516–520
13. Peng WX, Jiao LF, Gao HY, Qi Z, Wang QH, Du HM, Si YC, Wang YJ, Yuan HT (2010) J Power Sources 196:2841–2847
14. Kim K, Cho YH, Kam DW, Kim HS, Lee JW (2010) J Alloys Compd 504:166–170
15. Wu SH, Shiu JJ, Lin JY (2011) J Power Sources 196:6676–6681
16. Herle PS, Ellis B, Coombs N, Nazar LF (2004) Nat Mater 3:147–152
17. Kim CW, Park JS, Lee KS (2006) J Power Sources 163:144–150
18. Xu YB, Lu YJ, Yan L, Yang ZY, Yang RD (2006) J Power Sources 160:570–576
19. Ge YC, Yan XD, Liu J, Zhang XF, Wang JW, He XG, Wang RS, Xie HM (2010) Electrochim Acta 55:5886–5890
20. Wang XC, Huang YD, Jia DZ, Guo ZP, Ni D, Miao M (2010) Preparation and characterization of high-rate and long-cycle $LiFePO_4$/C nanocomposite as cathode material for lithium-ion battery. J Solid State Electrochem. doi:10.1007/s10008-010-1269-4
21. Liu HW, Tang DG (2008) Solid State Ionics 179:1897–1901
22. Gao F, Tang ZY (2008) Electrochim Acta 53:5071–5075
23. Fang XS, Li J, Huang KL, Liu SQ, Huang CH, Zhuang SX, Zhang JB (2011) Synthesis and electrochemical properties of K-doped $LiFePO_4$/C composite as cathode material for lithium-ion batteries. J Solid State Electrochem. doi:10.1007/s10008-011-1426-4
24. Fey TK, Huang KP, Kao HM, Li WH (2011) J Power Sources 196:2810–2818